



Research Article

Preparation and Evaluation of Onjisaponin B-Loaded Liposomes for Drug Delivery to Enhance Mitochondrial Function and Rescue Parkinson's Disease by Activating Mitophagy

Junhua Zhang,¹ Rui Bao ,² Faisal Raza ,³ Hajra Zafar ,³ Yingjie Qi,¹ Yurui Geng,¹ Ran Li,² Jianqin Xue,⁴ and Feng Shi ²

¹Department of Neurology, Jintan Hospital Affiliated to Jiangsu University, Changzhou 213200, Jiangsu, China

²School of Pharmacy, Jiangsu University, Zhenjiang 212013, Jiangsu, China

³School of Pharmacy, Shanghai Jiao Tong University, No. 800, Dongchuan Road, Shanghai 200240, China

⁴Department of Rehabilitation Medicine, Jintan Hospital Affiliated to Jiangsu University, No. 16, Nanmen Street, Jintan District, Changzhou 213200, Jiangsu, China

Correspondence should be addressed to Faisal Raza; faisalraza@sjtu.edu.cn and Feng Shi; shifeng_1985_wcl@163.com

Received 10 July 2023; Revised 24 October 2023; Accepted 30 October 2023; Published 8 November 2023

Academic Editor: Samuel Silvestre

Copyright © 2023 Junhua Zhang et al. This is an open access article distributed under the Creative Commons Attribution License, which permits unrestricted use, distribution, and reproduction in any medium, provided the original work is properly cited.

Onjisaponin B (OB) is the main active ingredient of Radix Polygalae with various bioactivities. However, the protective effect of OB in Parkinson's disease (PD) has not been fully studied. Liposomes are ideal nanocarriers for drugs targeting the brain. In this study, we investigated the therapeutic effect of OB-loaded liposomes (lip OB) on a 1-methyl-4-phenyl-1,2,3,6-tetrahydropyridine- (MPTP-) induced mouse model of PD and 1-methyl-4-phenylpyridinium- (MPP⁺-) induced cell model of PD. Our results showed that lip OB significantly ameliorated MPTP-induced motor deficits and dopaminergic neuron loss in vivo and prevented MPP⁺-triggered cell viability reduction and apoptosis in vitro. Lip OB also improved mitochondrial dysfunction in PD models by driving PINK1/Parkin-mediated mitophagy. Furthermore, silencing PINK1 compromised the beneficial effects of lip OB on MPP⁺-treated PC12 cells. These findings suggested lip OB mitigates Parkinsonism in vivo and in vitro by enhancing mitochondrial dysfunction through the PINK1/Parkin pathway of mitophagy, which provides a new possibility for treating PD.

1. Introduction

Parkinson's disease (PD) is the second most common neurodegenerative disorder that afflicts millions of people worldwide [1]. α -synuclein accumulation and Lewy body formation are the pathological hallmarks of PD and eventually cause severe dopamine depletion in the substantia nigra pars compact (SNpc) as well as motor defects, such as bradykinesia and motor rigidity [2]. To date, there is no cure for PD, and current therapy is limited to supportive care that partially relieves the symptoms [3].

Mitochondria are considered as the "powerhouse" of the cell, and their main function is to generate adenosine 5' triphosphate (ATP) at the mitochondrial electron transport chain (ETC) [4]. Mitochondria also mediate calcium

homeostasis, oxidative stress response, and programmed cell death [5]. Although the precise mechanism of PD pathogenesis remains elusive, mitochondrial dysfunction has been identified to have a vital role in the neurodegenerative process of PD [6]. Previous evidence suggests that high levels of mitochondrial DNA deletion occurred in the substantia nigra neurons from PD patients [7]. In addition, mitochondrial ETC inhibitors such as trichloroethylene and 1-methyl-4-phenyl-1,2,3,6-tetrahydropyridine- (MPTP-) induced parkinsonism in humans and experimental animals [5, 8].

Autophagy is a highly conserved cellular recycling process that serves to deliver cytoplasmic constituents to lysosomes for degradation, and plays important roles in cell survival and maintenance [9]. The selective degradation of

mitochondria by autophagy is termed as mitophagy, which eliminates dysfunctional mitochondria and prevents ATP deficiency and ROS accumulation resulting in oxidative stress and cell death [10]. PINK1 is a serine/threonine kinase localized at mitochondria, and Parkin is an E3 ubiquitin ligase resides in the cytosol [11]. The PINK1/Parkin-mediated mitophagy is the most studied mitophagy pathway. PINK1 detects damaged mitochondria and then recruits Parkin to ubiquitinate the dysfunctional mitochondria for their degradation by autophagy [12]. Previous studies have provided clear evidence to support the involvement of the PINK1/Parkin pathway of mitophagy in the pathogenesis and treatment of PD [13, 14].

Liposomes, fabricated from the self-assembly of phospholipids, have been widely used as a drug delivery system to the brain [15]. Depocyt is a cytarabine liposomal injection that is F.D.A. approved for the treatment of neoplastic meningitis through spinal injection [16]. Depocyt could treat neoplastic meningitis with the controlled release of Ara-C. Kasenda et al. carried out evaluation of targeted immunoliposomes for the treatment of epidermal growth factor receptor- (EGFR-) positive glioblastoma by clinical trial. They found that anti-EGFR immunoliposomes can target EGFR-amplified glioblastoma [17]. As an ideal nanocarriers for the central nervous system, liposomes improve the bioavailability of drugs and minimize systemic effects of drugs by enhancing BBB penetration, targeting a specific group of cells, and avoiding premature metabolism [18]. Onjisaponin B (OB) is an active compound derived from *Radix Polygalae*, which exerts neuroprotective effects in neurodegenerative disorders, such as AD and PD [19, 20]. Existing evidence shows that OB successfully ameliorated DA neurons degeneration and motor deficits by enhancing autophagy and decreasing oxidative stress in a mouse model of PD [19, 21]. OB was also demonstrated to promote the clearance of α -synuclein mutants (a central component to the pathogenesis of PD) in PC12 cells via autophagy activation [22]. However, the therapeutic effect of OB-loaded liposomes has not been studied.

Liposomes as drug carriers have the following three main advantages: (1) simplified manufacturing method, (2) ability to encapsulate a wide range of drugs and molecules and are not limited by other physicochemical properties such as hydrophobicity and charge, and (3) biocompatibility. In the aqueous environment, the hydrophobic tail forms a spherical structure composed of an aqueous core, which is surrounded by a lipophilic bilayer membrane. Liposomes can be controlled by changing the lipid composition because they are biocompatible and biodegradable. In addition, liposomes can be subjected to various modifications to enhance their efficacy as drug delivery carriers.

To address this issue, the present study explored the effects of lip OB in cell and mouse models of PD. We found that lip OB rescued motor defects, dopaminergic neurons degeneration in vivo, and improved cell survival in vitro. Furthermore, these effects are related to the restoration of mitochondria dysfunction by activating the PINK1/Parkin signaling of mitophagy.

2. Results

2.1. Lip OB Rescues MPTP-Induced Motor Deficits and Dopaminergic Neurons Degeneration In Vivo. MPTP is a neurotoxin that can induce PD symptoms in humans and rodent animals by metabolizing into 1-methyl-4-phenylpyridinium (MPP^+) that enters dopaminergic neurons, where it inhibits respiratory chain complexes [23]. To evaluate the protective effects of lip OB on PD, an MPTP-induced PD mouse model was employed. Following administration with free or lip OB, the latency to fall (MPTP: 158.9 ± 21.12 s, MPTP + free OB: 183.0 ± 18.79 s, MPTP + lip OB: 212.5 ± 10.98 s, Control: 222.0 ± 9.506 s) in the rotarod test was significantly increased, and the time spent turning around (MPTP: 3.489 ± 0.3951 s, MPTP + free OB: 2.800 ± 0.4183 s, MPTP + lip OB: 2.133 ± 0.4924 s, Control: 2.078 ± 0.4381 s) and climbing down (MPTP: 13.01 ± 1.101 s, MPTP + free OB: 11.14 ± 1.467 s, MPTP + lip OB: 9.078 ± 1.287 s, Control: 7.078 ± 1.039 s) in the pole test were evidently decreased relative to the MPTP group (Figures 1(a)–1(c)).

Next, we examined lip OB-induced effects on dopaminergic degeneration in the SNpc (Figure 1(d)). As expected, TH-positive cells in the MPTP group were greatly reduced as compared to those in the controls. However, free or lip OB treatment greatly inhibited the death of TH-positive neurons (MPTP: 4522 ± 1181 , MPTP + free OB: 7553 ± 447.2 , MPTP + lip OB: 8397 ± 1024 , Control: 11107 ± 1530). It is noteworthy, that lip OB showed better effects than free OB on mitigating MPTP-induced behavioral dysfunction and dopaminergic neurons loss. Collectively, these results suggest that lip OB could ameliorate PD-related motor impairments and dopaminergic neurons degeneration.

2.2. Lip OB Remedies MPTP-Induced Mitochondrial Dysfunction In Vivo. Mitochondrial dysfunction is tightly linked to PD pathogenesis [24]. Mitochondrial Complex I is the largest multimeric enzyme complex of the mitochondrial respiratory chain, the inhibition of which leads to ATP depletion and ROS generation responsible for oxidative stress [25]. Complex I deficiency has been reported in PD patients [24, 26]. To explore the role of OB in mitochondrial function, we detected the levels of Complex I, ATP, and oxidative stress. As shown in Figure 2, MPTP treatment reduced the activities of Complex I and ATP and elevated the generation of MDA and SOD. Nonetheless, the aforementioned effects were all successfully reversed by lip OB administration. In contrast, free OB only significantly rescued the SOD levels. These results indicated that lip OB restores MPTP-induced mitochondria dysfunction.

2.3. Lip OB Induces Mitophagy by Activating PINK1/Parkin Pathway. Mitophagy is a selective form of autophagy, which controls mitochondrial quality by removing damaged mitochondria and is involved in the pathology of Parkinson's disease [13, 27]. The PINK1/Parkin pathway is reported to play an essential role in triggering mitophagy [28]. We thus investigated whether OB-induced improvement in mitochondria function is associated with PINK1/Parkin

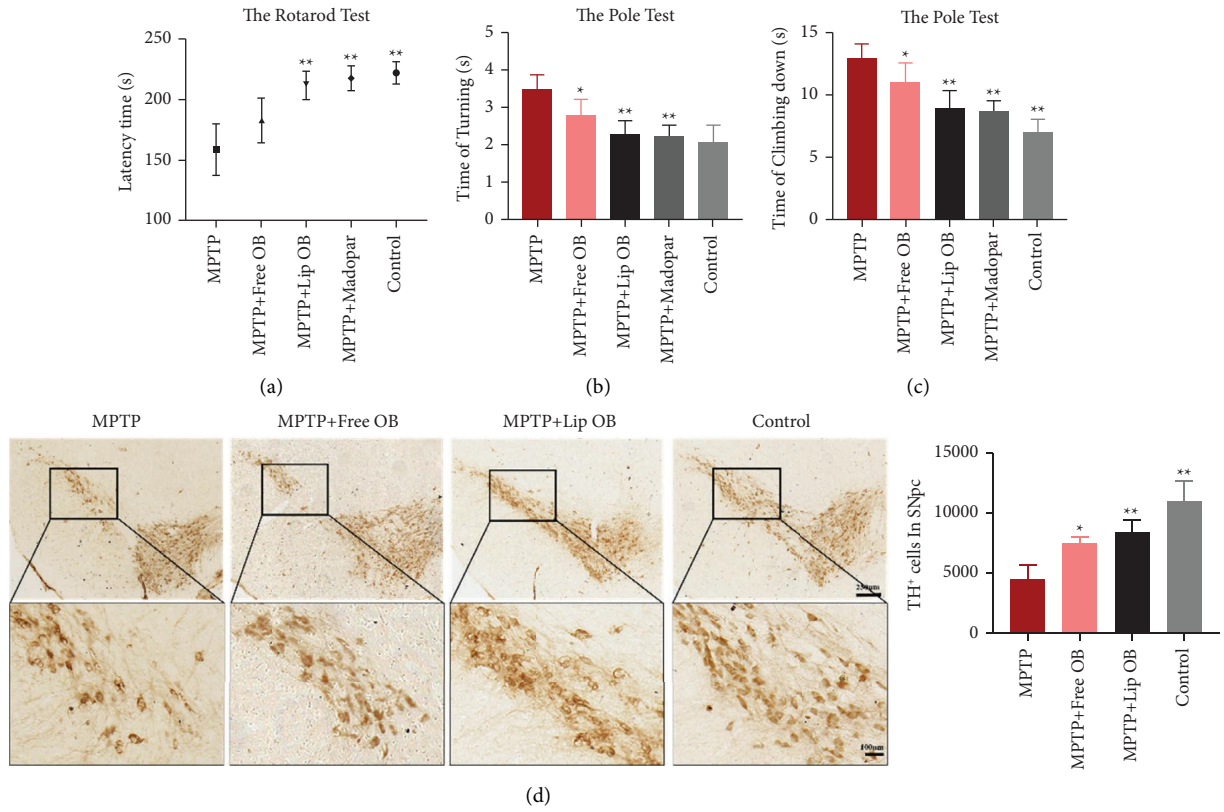


FIGURE 1: Lip OB reduces motor impairments and dopaminergic neuronal loss in mice exposed to MPTP. (a) Latency to fall in the rotarod test ($n = 9$). (b, c) Time of turning downward and reach the bottom in the pole test ($n = 9$). (d) Representative pictures and quantification of TH+ neurons in the SNpc of mice exposed to MPTP ($n = 3$). Scale bar: $100 \mu\text{m}$. Data were expressed as means \pm SD. * $P < 0.05$, ** $P < 0.01$ compared with MPTP group.

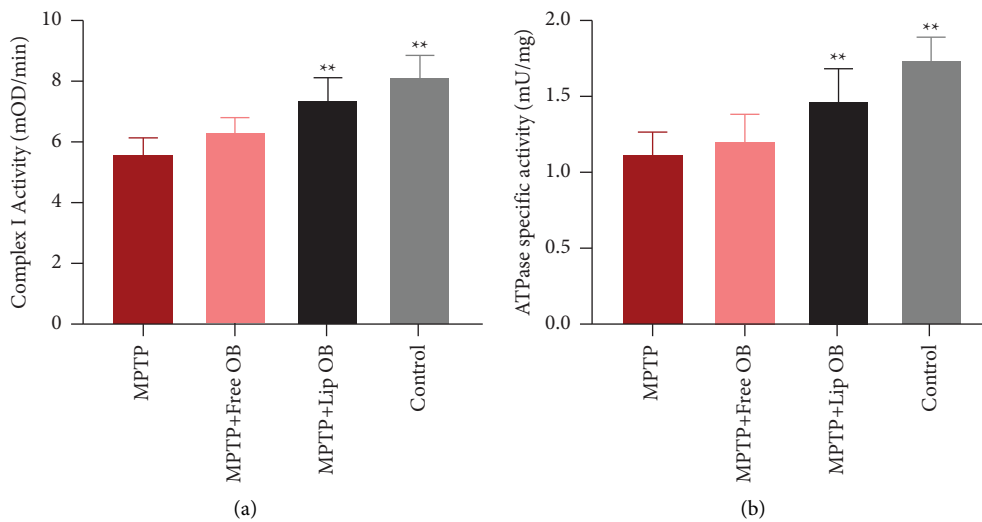


FIGURE 2: Continued.

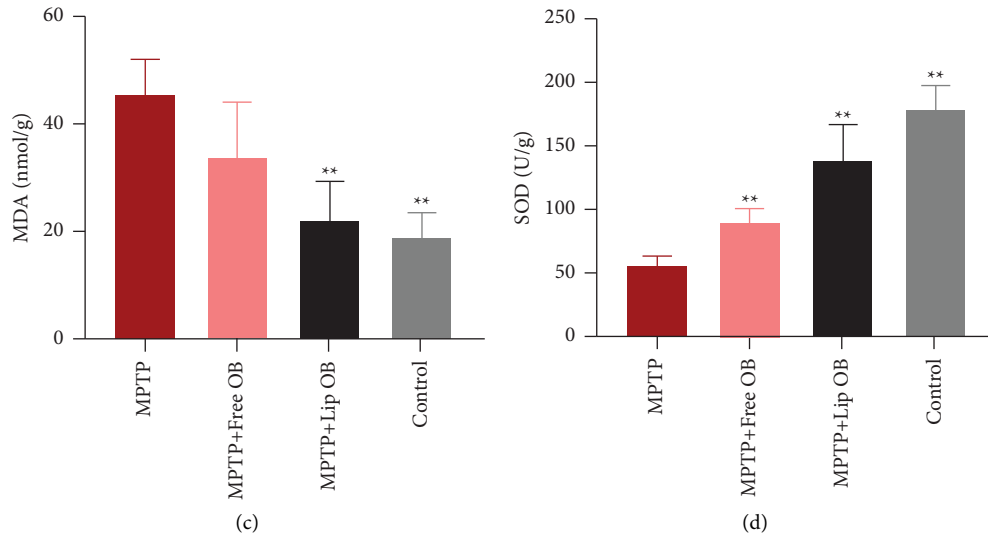


FIGURE 2: Lip OB improves mitochondrial dysfunctions in mice exposed to MPTP. The levels of Complex I, ATP, MDA, and SOD in the SNpc were determined using the commercial kits. Data were expressed as means \pm SD ($n = 6$). ** $P < 0.01$ compared with the MPTP group.

dependent mitophagy. During autophagy, ATG5 and LC3-I to LC3-II conversion are involved in autophagosome formation [29]. LAMP2A locates in the lysosomal membrane and is responsible for the protein translocation from the cytosol to the lysosomal lumen [30]. P62 is an autophagosome cargo protein that is critical for the clearance of ubiquitinated proteins [30]. In the western blotting, MPTP-induced a notable decrease in PINK1 and Parkin expression, accompanied by a significant reduction in ATG5 expression, LC3-II/LC3-I ratio and LAMP2A levels, and an increase in P62 expression (Figure 3). Interestingly, these effects were all reversed after treatment with lip OB, while free OB only rescued the protein levels of ATG5 and P62. Together, these data suggest that lip OB activates PINK1/Parkin-mediated mitophagy in the PD mouse model.

2.4. Lip OB Improves Cell Survival and Mitochondrial Function in MPP⁺-Treated PC12 Cells through PINK1/Parkin Pathway of Mitophagy. To explore the beneficial effects of lip OB on Parkinson's disease in vitro, PC12 cells were pre-treated with lip OB for 6 h, followed by exposure to MPP⁺ for 24 h. Given that the maximum concentration that had no effect on decreasing cell viability was 0.8 μ M for lip OB, this dose was chosen as the high dose in in vitro experiments (Figure 4(a)). As shown in Figures 4(b)–4(d), lip OB alleviated MPP⁺-induced cell viability reduction (MPP⁺: 61.56 \pm 7.751%, MPP⁺ + 0.2 μ M: 74.60 \pm 4.947%, MPP⁺ + 0.4 μ M: 79.26 \pm 9.155%, MPP⁺ + 0.8 μ M: 86.89 \pm 4.902%, Control: 100.0 \pm 6.738%) and apoptosis (MPP⁺: 17.49 \pm 0.5838%, MPP⁺ + 0.2 μ M: 13.82 \pm 0.6817%, MPP⁺ + 0.4 μ M: 13.09 \pm 0.5565%, MPP⁺ + 0.8 μ M: 10.53 \pm 0.5216%, Control: 7.770 \pm 0.5963%) in a dose-dependent manner in PC12 cells.

The mitochondrial function was assessed by evaluating the mitochondrial respiration, mitochondrial membrane potential, and ROS generation. The oxygen consumption rate (OCR) data demonstrated that MPP⁺ suppressed

basal respiration, ATP production, maximal respiration, and spare capacity in PC12 cells (Figures 5(a) and 5(b)). However, lip OB ameliorated the results. Also, weakened mitochondrial membrane potential (reduced JC-1 aggregate/monomer percentage; Figure 5(c)) and increased ROS production (Figure 5(d)) were detected following MPP⁺ treatment, which were recovered by lip OB administration.

We next tested whether PINK1/Parkin-mediated mitophagy was involved in lip OB-generated beneficial effects in Parkinson's disease in vitro. In line with in vivo results, lip OB successfully blocked MPP⁺-induced increase in P62 expression and a decrease in PINK1, Parkin, ATG5, and LAMP2A levels, as well as LC3-II/LC3-I ratio (Figures 6(a) and 6(b)). The GFP-LC3-mitochondria colocalization showed that lip OB attenuated MPP⁺-induced loss in the colocalization of GFP-LC3 and mitochondria (Figure 6(c)).

Overall, these findings suggested that the damaging effects of MPP⁺ on neuronal survival and mitochondrial function were well restored with lip OB administration by affecting the PINK1/Parkin pathway of mitophagy.

2.5. Silencing PINK1 Abrogated the Protective Effects of Lip OB on MPP⁺-Treated PC12 Cells. To investigate whether the PINK1 pathway was required in the protective effect of lip OB against Parkinson's disease, PINK1 siRNA knockdown was performed in PC12 cells. As illustrated in Figures 7(a) and 7(b), PINK1 knockdown successfully abolished lip OB-induced effects on Parkin and autophagic protein levels in MPP⁺-treated PC12 cells. In addition, the beneficial effects of lip OB on cell viability reduction (scramble siRNA + vehicle: 59.44 \pm 3.290%, scramble siRNA + OB: 84.68 \pm 6.005%, PINK1 siRNA + vehicle: 47.74 \pm 3.005%, PINK1 siRNA + OB: 55.95 \pm 6.631%), apoptosis (scramble siRNA + vehicle: 18.71 \pm 1.690%, scramble siRNA + OB:

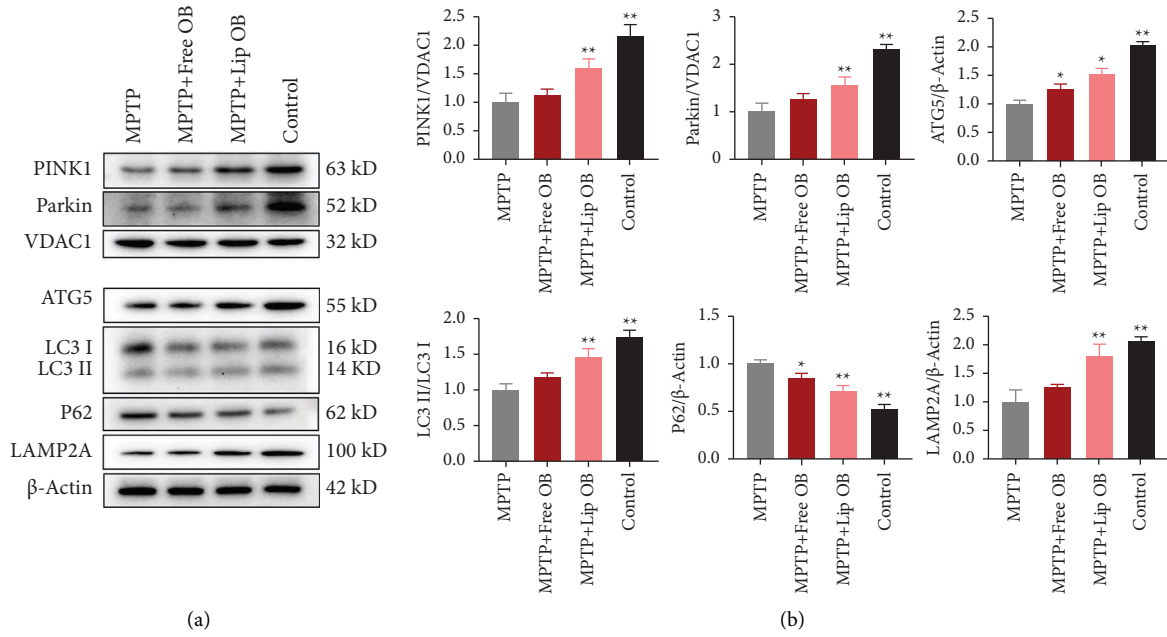


FIGURE 3: Lip OB enhances PINK1/Parkin pathway of mitophagy in mice exposed to MPTP. (a) Representative images of mitophagy in the western blot analysis. (b) Quantitation of PINK1, Parkin, ATG5, LC3, P62, and LAMP2 levels in the SNpc. Data were expressed as means ± SD ($n = 3$). * $P < 0.05$, ** $P < 0.01$ compared with the MPTP group.

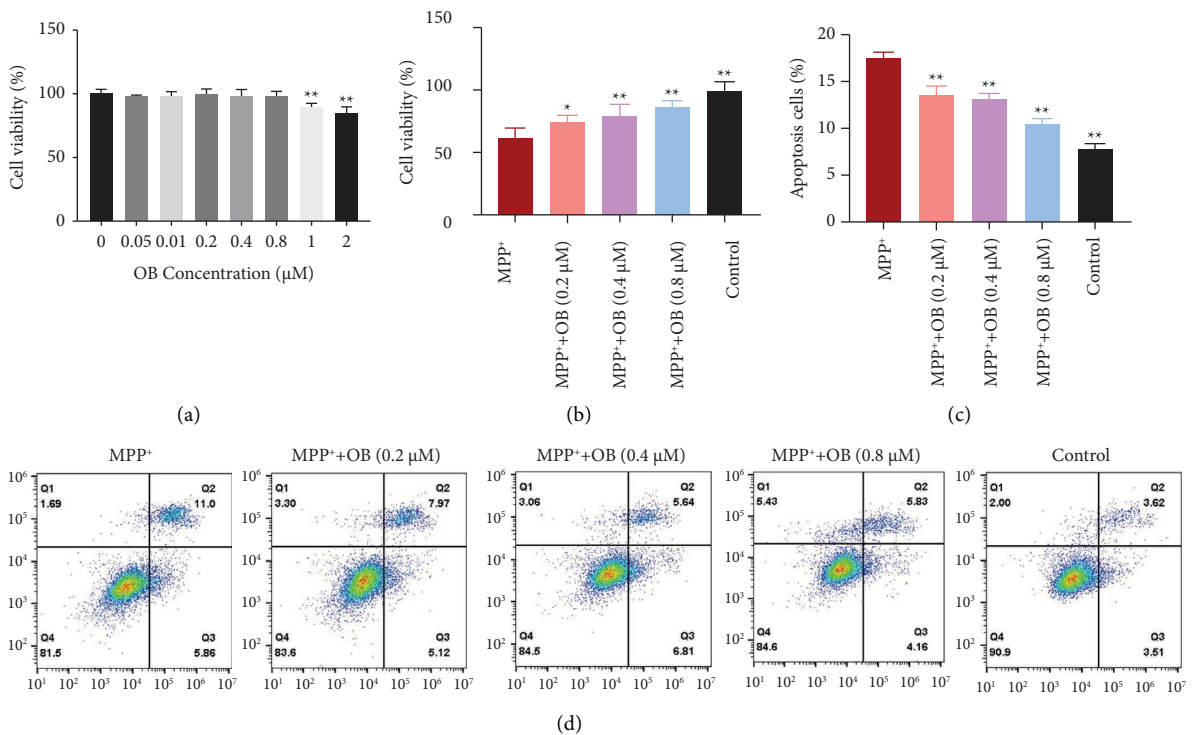
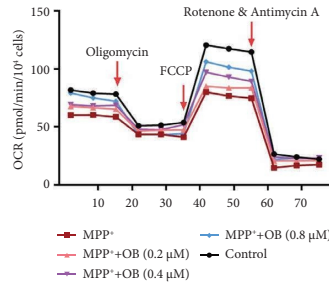
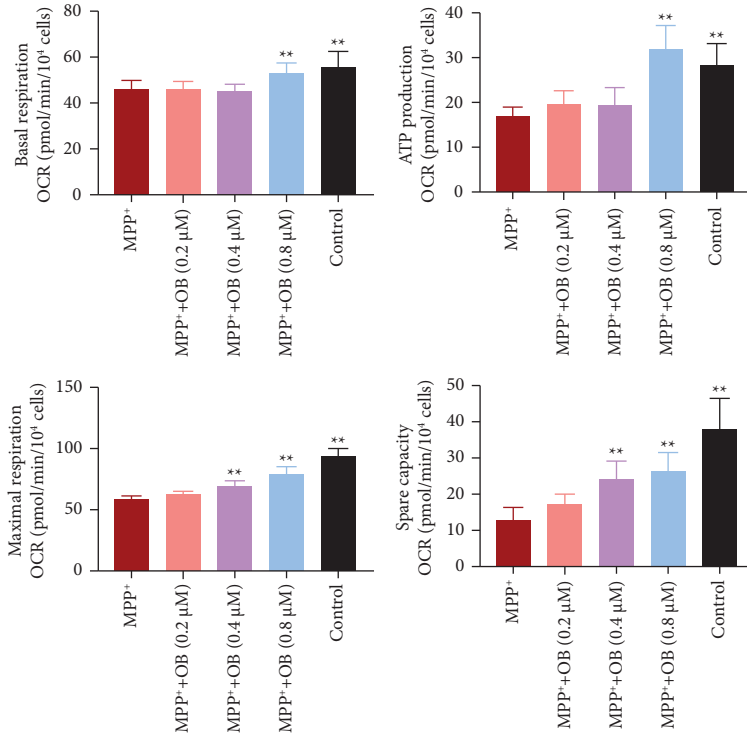


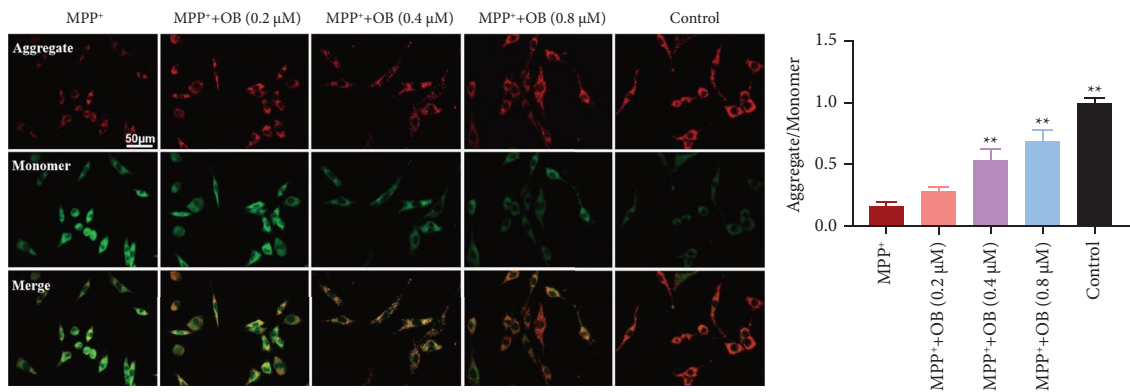
FIGURE 4: Lip OB inhibits cell survival in MPP⁺-treated PC12 cells. (a) Screening of lip OB concentrations using the MTT assay ($n = 5$). (b) PC12 cells were pretreated with lip OB for 6 h, followed by the exposure to MPP⁺ for 24 h. The cell viability was detected by the MTT assay ($n = 5$). (c, d) Flow cytometry analysis of the apoptosis ratio of PC12 cells ($n = 3$). Data were expressed as means ± SD. * $P < 0.05$, ** $P < 0.01$ compared with blank or MPP⁺ group.



(a)



(b)



(c)

FIGURE 5: Continued.

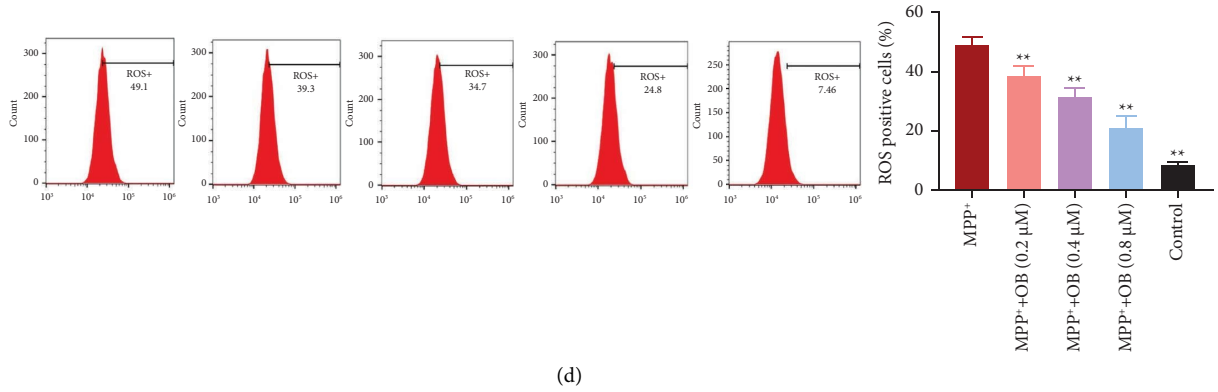


FIGURE 5: Lip OB improves mitochondrial defects in MPP⁺-treated PC12 cells. (a, b) The influence of lip OB on mitochondrial respiration, including basal and maximal respiration, ATP production, and spare capacity, was analyzed using a Seahorse XFe96 analyzer (*n* = 6). (c) Mitochondrial membrane potential level of PC12 cells detected by the JC-1 staining (*n* = 3). (d) Intracellular ROS generation in MPP⁺-treated PC12 cells measured using DCF-DA and flow cytometry (*n* = 3). Data were expressed as means ± SD. * *P* < 0.05, ** *P* < 0.01 compared with MPP⁺ group.

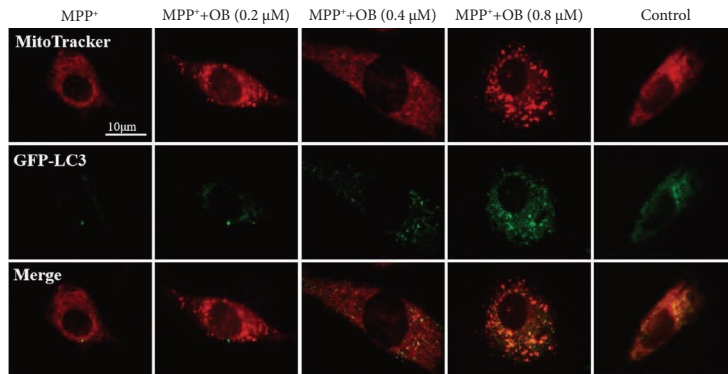
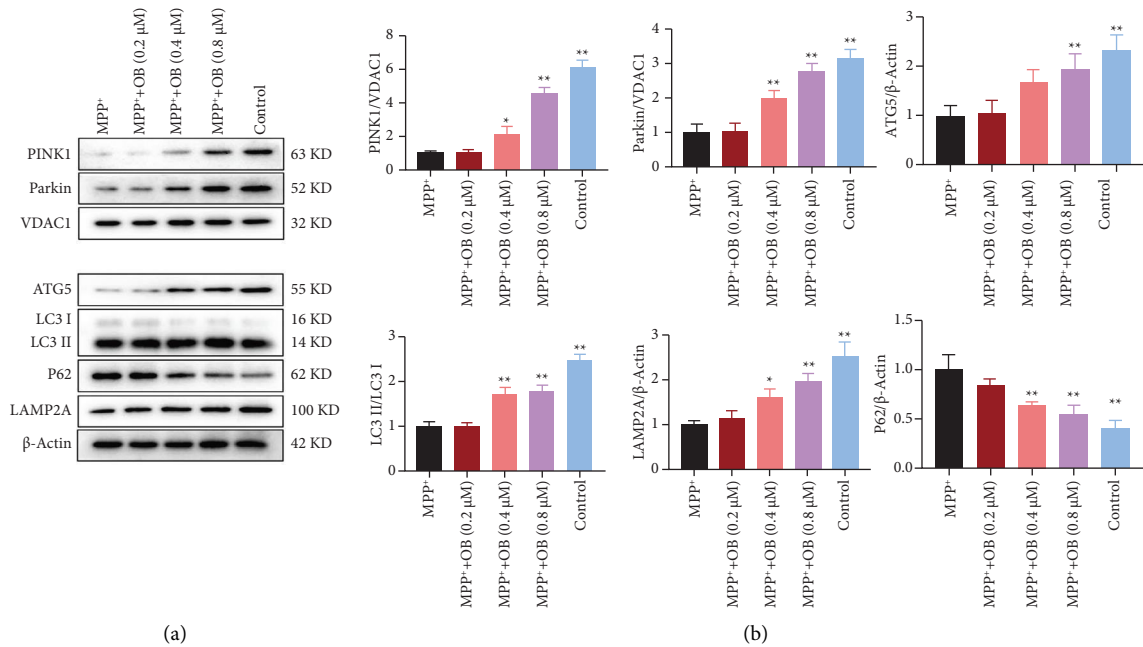


FIGURE 6: Lip OB activates PINK1/Parkin pathway of mitophagy in MPP⁺-treated PC12 cells. (a) Representative images of mitophagy in the western blot analysis. (b) Quantitation of PINK1, Parkin, ATG5, LC3, P62, and LAMP2 levels in PC12 cells. (c) Representative confocal images of mitochondria (red) and GFP-LC3 (green) depicting colocalization of mitochondria and GFP-LC3. Data were expressed as means ± SD (*n* = 3). * *P* < 0.05, ** *P* < 0.01 compared with MPP⁺ group.

7.920 ± 0.9560%, PINK1 siRNA + vehicle: 18.23 ± 2.640%, PINK1 siRNA + OB: 14.27 ± 3.172%), and mitochondrial functions (mitochondrial membrane potential and ROS production) in MPP⁺-treated PC12 cells were also disappeared after silencing PINK1 (Figures 7(c)–7(g)). These data indicated that the PINK1 pathway is required in lip OB-induced protective effects in Parkinson disease.

3. Discussion

PD is a common neurodegenerative disorder that is clinically characterized by tremor, gait rigidity, and hypokinesia [31]. The morbidity of PD presents significant healthcare, social, and economic issues [32]. However, there is no available treatment that can halt the progression of the disease. In the present study, we investigated the therapeutic effect of OB-loaded liposomes on PD. We found that lip OB significantly reduced the motor impairment and dopaminergic neuron loss in PD models. In addition, enhancement of mitochondrial function was observed following lip OB treatment, which was associated with PINK1/Parkin signaling-mediated mitophagy.

OB is a major component from the herbal medicine *Radix Polygalae*. OB possesses strong biological activities and has displayed therapeutic effects in several disease models, including PD [21, 33, 34]. In our work, OB rescued MPTP-induced motor dysfunction and dopaminergic neuron death in a mouse model of PD, confirming the protective role of OB in PD. Furthermore, lip OB displayed a better effect on ameliorating Parkinson-like syndrome relative to free OB, supporting the strength of liposomes served as a drug delivery system to the brain.

Mitochondria are the main sites of biological energy generation in eukaryotes and regulate a wide variety of cellular functions, including ATP production, calcium buffering, ROS production, and scavenging [35]. Mounting evidence suggests that mitochondria play an important role in PD [36, 37]. For example, mitochondrial respiratory chain deficiency such as reduced Complex I activities was seen in the skeletal muscle, platelets, and substantia nigra of patients with PD [38]. Postmortem studies have shown high levels of oxidation of lipids and proteins in the substantia nigra of PD brains [39]. Andrographolide restored mitochondrial functions by inhibiting mitochondrial excessive division, which ultimately mitigated Parkinsonism in MPTP-PD mice [40]. Consistent with these studies, we found that MPTP or MPP⁺ modeling impaired mitochondrial respiration and mitochondrial membrane potential and aggravated ROS accumulation and oxidative stress response, suggesting the involvement of mitochondrial dysfunction in PD. While treatment with lip OB attenuated PD symptoms by enhancing mitochondrial functions, it highlighted the critical role of mitochondria restoration in the treatment of PD.

Mitochondria selective autophagy, termed as mitophagy, is a mechanism of elimination of mitochondria via autophagy, and mediates mitochondrial quality control and homeostasis [41]. In mammalian cells, the mitochondrial kinase PINK1 and the E3 ubiquitin ligase Parkin act in coordination in monitoring mitochondrial functional state

and tags damaged mitochondria for autophagic clearance [42]. The alternation of PINK1/Parkin-mediated mitophagy in PD has been documented in previous studies [12, 43]. Mutations in the PINK1 and Parkin result in autosomal recessive and juvenile parkinsonism [44, 45]. δ -opioid receptor (DOR) activation rescued PD-related mitochondrial damage by driving the PINK1/Parkin pathway of mitophagy. While knockdown of PINK1 aggravated mitochondrial dysfunction and compromised DOR-induced cytoprotection against MPP⁺ [46]. Huang et al. found that vasicinone suppressed ROS production, improved mitochondrial membrane potential, and prevented paraquat-induced PD through enhancing mitophagy; however, inhibition of mitophagy abolished the ameliorating effect of vasicinone in PD [47]. In our study, the PINK1/Parkin pathway of mitophagy was suppressed in the cell and mouse models of PD and was successfully activated following lip OB treatment. Furthermore, PINK1 siRNA knockdown blocked lip OB-generated therapeutic effects in PD. These findings supported the importance of PINK1/Parkin-mediated mitophagy in the etiology and treatment of PD.

In conclusion, this study demonstrated that lip OB plays a protective role in PD by enhancing mitochondria function via PINK1/Parkin-mediated mitophagy. Our study shows the potential of lip OB in treating PD.

4. Materials and Methods

4.1. Preparation and Characterization of OB-Loaded Liposomes. OB-loaded PEG/cyclic Arg-Gly-Asp (cRGD) dual-modified liposomes were prepared using the thin-film dispersion method [48]. Briefly, SPC, cholesterol, PEG-DSPE, and SH-PEG-DSPE were dissolved at a molar ratio of 80:15:3:2 in chloroform. This mixture was rotated in a rotary evaporator at 37 ± 5°C for 10 min. The thin film was dissolved in chloroform and mixed with a 120 mmol/L calcium acetate solution (pH 7.3). Liposomes were sonicated at 300 W, 5 min in an ice bath, and then filtered through a 220 nm pore size polycarbonate membrane. Liposomes preformed in calcium acetate solution (inside pH 7.3) were rinsed twice in 120 mmol/L sodium sulfate solution (outside pH 5.9) by ultracentrifugation at 100 000 × *g* and 4°C for 60 min. Afterwards, onjisaponin B (>98% purity; MUST Bio-technology) in 120 mmol/L sodium sulfate solution was added. Liposomes were then ultracentrifuged at 100 000 × *g* and 4°C for 60 min. Finally, the liposomes were incubated with the Mal-cRGDyk peptide at an equimolar amount of SH-PEG-DSPE at 37°C for 2 h.

The morphology of the prepared liposomes was observed under a transmission electron microscopy (HT7700, HITACHI; Figure S1A). The size distribution and zeta potential of liposomes were determined using a Nano ZS90 Zetasizer (Figures S1B and S1C).

To determine the body biodistribution profile of lip OB, C57BL/6J mice were injected with MPTP (30 mg/kg) twice a week for 3 weeks. At 6 h post the last MPTP treatment, DiR-labeled liposomes including Lip, Lip-PEG, Lip-cRGD, and Lip-PEG-cRGD were given to mice by intravenous injection. At 12 h postliposome administration, the images

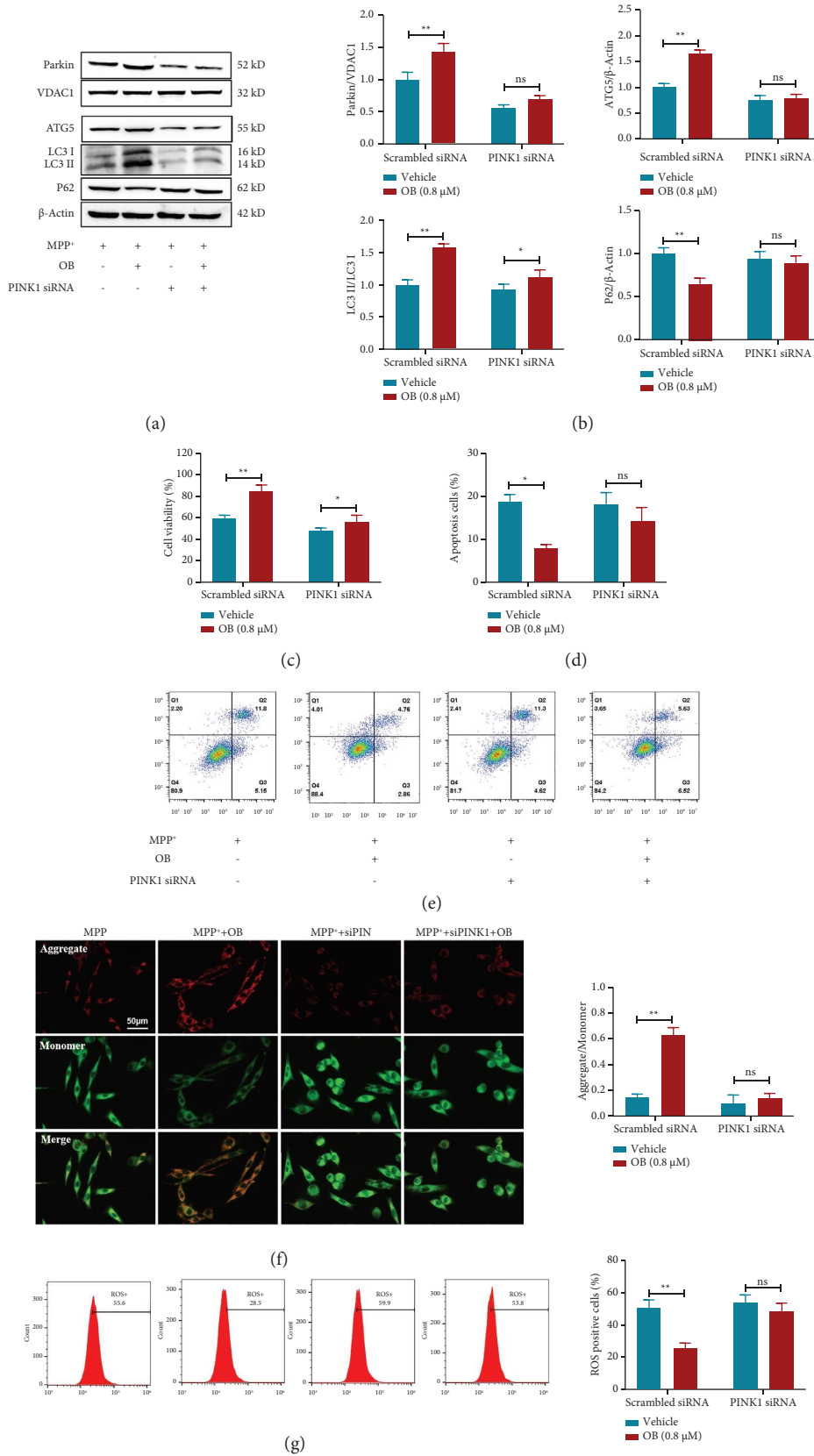


FIGURE 7: PINK1 inhibition compromised the protective effects of lip OB in MPP⁺-treated PC12 cells. (a, b) Representative gels of mitophagy in the western blot analysis. (b) Quantitation of Parkin, ATG5, LC3, and P62 levels in PC12 cells ($n = 3$). (c) Cell viability of PC12 cells determined by the MTT assay ($n = 5$). (d, e) Flow cytometry analysis of the apoptosis rate of PC12 cells ($n = 3$). (f) Mitochondrial membrane potential levels of PC12 cells detected by the JC-1 staining ($n = 3$). (g) Intracellular ROS generation in MPP⁺-treated PC12 cells measured using DCF-DA and flow cytometry ($n = 3$). Data were expressed as means \pm SD. * $P < 0.05$, ** $P < 0.01$; ns, not significant.

of the mice were derived using the fluorescence imaging system IVIS Lumina II (IVIS; Figure S1D). Hereafter, mice were euthanized, and the brains were harvested and imaged using the IVIS.

4.2. Animals Experiments. C57BL/6 mice at 3 months of age were purchased from Shanghai Sipper-BK Laboratory Animal Co. Ltd (Shanghai, China). The animals were group-housed and maintained under a 12-hour light/dark cycle with free access to food and water. The animals were managed according to procedures approved by Jiangsu University.

After a week of acclimatization, mice were divided into four groups at random ($n=9$ per group): control, MPTP, MPTP + free OB, and MPTP + lip OB groups. MPTP (30 mg/kg/day; Sigma) was given by intraperitoneal (i.p.) injection twice a week for 3 weeks. At 6 h post the last MPTP treatment, free and lip OB were administered (i.v.) at a dose of 5 mg/kg. The control group received i.v. and i.p. injections of the same dose of normal saline. The MPTP group received i.p. injection of MPTP and i.v. administration of the same dose of normal saline. Twelve hours after OB treatment, the rotarod test and pole test were performed subsequently. Afterwards, mice were euthanized by cervical dislocation for tissues sampling.

4.3. Cell Culture and Treatment. The PC12 cell line was obtained from the Cell Bank of the Chinese Academy of Sciences (Shanghai, China) and cultured in Dulbecco's modified Eagle medium containing 10% fetal bovine serum (FBS; Gibco) and 1% antibiotic at 37°C in a humidified atmosphere containing 5% CO₂. Cells were treated with 0.2–0.8 μM of free or lip OB for 6 h, followed by exposure to 5 μM MPP⁺ (Sigma) for 24 h. For gene knockdown, the cells were transfected with PINK1 siRNA prior to OB administration as described below. The MPP⁺ concentration and OB treatment time window were determined by the MTT and western blotting assays, respectively (Figure S2).

4.4. RNA Interference of PINK1. To inhibit of PINK1 expression, PC12 cells seeded in 6-well plates were transfected with specific PINK1 siRNA for 12 h using the Lipofectamine 3000 according to the manufacturer's instructions. The transfection efficiency was evaluated by the western blot analysis (Figure S3).

4.5. Rotarod Test. Motor balance and coordination were evaluated using a rotarod apparatus as previously described [49]. Mice underwent two trails (6 min per trail, with an accelerated speed of 12–20 rpm) per day for 2 consecutive days prior to the assessment. Then, the animals were tested for 5 min (constant 20 rpm). The latency to fall off the rotating rod was recorded as latency time. A decreased latency time is associated with a motor deficit.

4.6. Pole Test. The pole test was conducted to measure bradykinesia as reported previously [49]. The apparatus consisted of a rough-surfaced wooden pole (50 cm in height, 1 cm in diameter) with a ball placed on top. The base of the pole was covered with bedding to protect mice from injury. Mice were positioned upward at the top of the pole. The time required for the mice to completely turn downward and reach the bottom was recorded. All mice were pretrained with the pole three times prior to the assessment.

4.7. Immunohistochemical Analysis. The technique we used was performed as reported previously [50]. Sections were washed in PBS, permeabilized in 0.5% Triton X-100 for 10 min, followed by incubation in 3% H₂O₂ for 20 min. After that, brain slices were blocked with a 5% bovine serum albumin (BSA) solution for 1 h and incubated with an antibody against TH overnight at 4°C. The following day, sections were incubated with the corresponding secondary antibodies at room temperature for 2 h. Then, the slices were stained with 3,3'-diamino-benzidine (DAB), mounted on glass slides, and coverslipped. Digital images of TH neurons in SNpc were captured using an Olympus BX52 microscope.

4.8. Measurement of Complex I, ATP, MDA, and SOD. The levels of Complex I (ab109721, Abcam), ATP (S0026, Beyotime), MDA (A003-1-2; Nanjing Jiancheng Bioengineering Institute), and SOD (A001-3-2; Nanjing Jiancheng Bioengineering Institute) in mice were determined using the corresponding kits following the manufacturer's protocol.

4.9. Western Blotting. The western blotting analysis was performed according to a previously described protocol [51]. Briefly, brain tissues and cells were lysed in RIPA buffer containing protease and phosphatase inhibitors. The concentrations of proteins were determined by a BCA protein assay kit. Equal amounts of proteins were separated by sodium dodecylsulfate-polyacrylamide gel electrophoresis (SDS-PAGE) and transferred to polyvinylidenedifluoride (PVDF) membranes. After blocking with 5% BSA for 1 h, the blots were incubated with primary antibodies against PINK1 (DF7742, Affinity), Parkin (AF0235, Affinity), ATG5 (DF6010, Affinity), LC3 A/B (ab128025, Abcam), P62 (39749, CST), and LAMP2A (ab125068, Abcam) overnight at 4°C. Antibodies to VDAC1 (DF6140, Affinity) and β-Actin (AF7018, Affinity) were used as loading control for mitochondrial and total proteins, respectively. The next day, the appropriate horseradish peroxidase (HRP)-conjugated secondary antibody (ab7090, Abcam) was added for further incubation for 90 min at room temperature. The protein bands were visualized with enhanced chemiluminescence reagents (ECL), and their densities were quantified using ImageJ (NIH). Tissue and cell mitochondrial extraction was performed using the mitochondrial isolation kit (C3606, C3601, and Beyotime) following the manufacturer's protocols.

4.10. MTT. Cell viability was evaluated by the 3-(4,5-dimethylthiazol-2-yl)-2,5-diphenyltetrazolium bromide the (MTT) assay. Cells were plated in 96-well plates at a density of 5×10^3 cells per well. After pretreatments with MPP⁺, OB, or MPP⁺ plus OB, MTT was added and cultured at 37°C for 4 h, followed by exposure to DMSO. The optical density (OD) was analyzed at 570 nm on a Microplate Reader (Thermo Scientific, USA).

4.11. Flow Cytometric Detection of Apoptotic Cells. The Annexin V-FITC apoptosis detection kit (C1062S, Beyotime) was used to assess cell apoptosis in accordance with the manufacturer's instruction. Briefly, after treatment, cells were harvested, washed with ice-cold PBS, and resuspended with binding buffer. Next, cells were incubated with Annexin V-FITC (5 μ L) and PI (5 μ L) at room temperature for 15 min. Finally, the cell apoptotic rate was measured by a BD-LSR flow cytometer using the CellQuest software.

4.12. Seahorse Respiration Assay. The mitochondrial oxygen consumption rate was measured using a Seahorse XFe96 extracellular flux analyzer as previously described. Briefly, cells were seeded at 5×10^3 cells/well in the XFe96-well cell culture microplate till they reached 80% confluency. Then, OB was added to the media for 6 h, followed by MPP⁺ exposure for 24 h. Basal respiration was measured before the sequential injection of the following inhibitors: oligomycin (1 μ M), FCCP (1 μ M), and rotenone and antimycin A (1 μ M).

4.13. Mitochondrial Membrane Potential (MMP) Assay. A JC-1 kit (Invitrogen) was used to observe the mitochondrial potential. Cells were incubated with a diluted JC-1 reagent (1 : 1000) at 37°C for 20 min. After rinsing with PBS, cells were observed under a fluorescence microscope. At a high MMP, JC-1 forms aggregates (red fluorescence; 550 nm excitation/600 nm emission) inside mitochondria, whereas in a low MMP state, JC-1 remains as a monomer (green fluorescence; 485 nm excitation/535 nm emission). The ratio of fluorescence red/green fluorescence intensity was quantified using the ImageJ software (NIH).

4.14. Determination of ROS Production. The ROS probe dye 2',7'-dichlorofluorescein diacetate (DCF-DA) was used to determine intracellular ROS generation. Cells were loaded with 10 μ M DCF-DA for 30 min and then rinsed in PBS twice. Fluorescent signal detection of cells was performed using a flow cytometry.

4.15. LC3B-GFP-Adenoviral Transfection. LC3B-GFP-adenoviral transfection and MitoTracker Red staining were performed to visualize mitophagy as previously documented [52]. PC12 cells were transfected with GFP-LC3B adenovirus for 24 h, treated with OB (0.2, 0.4, and 0.8 μ M) for 6 h, and then exposed to 5 μ M MPP⁺ for another 24 h. After washing in PBS, cells were stained with MitoTracker Red (500 nM, CST) at 37°C for 30 min to visualize mitochondria. Then,

cells were washed with PBS and fixed in 4% paraformaldehyde for 15 min. Images were captured using a Leica confocal microscope.

4.16. Statistical Analysis. Data were presented as the mean \pm standard deviation (SD). Comparison between two groups was analyzed using an unpaired two-tailed *t* test. Differences among multiple groups were determined using one- or two-way analysis of variance (ANOVA), followed by a post hoc test (Dunnett's or Sidak's multiple comparisons tests). Statistics were conducted using the GraphPad Prism 8 software. The criterion of significance was set at $P < 0.05$.

Data Availability

The data presented in this study are available on request from the corresponding author.

Ethical Approval

Research experiments conducted in this article with animals or humans were approved by the Ethical Committee and responsible authorities of Jiangsu University (UJS-IACUC-2021031202), following all guidelines, regulations, legal, and ethical standards as required for humans or animals.

Conflicts of Interest

The authors declare that there are no conflicts of interest.

Authors' Contributions

J.Z. and H.Z. conceptualized the study. J.Z. Y.G., and J.X. contributed to the methodology. Y.Q. provided software. Y.G. performed validation. J.Z. R.B., R.L., and J.X. performed formal analysis. R.B. and F.S. contributed to data curation. J.Z. and F.R. wrote the original draft. J.Z. and F.S. wrote, reviewed, and edited the article. All authors have read and agreed to the published version of the manuscript.

Acknowledgments

The authors greatly appreciate all authors. This project was supported by the Changzhou Science and Technology Planning Project (CJ20220162).

Supplementary Materials

Figure S1. Characterizations of OB-loaded liposomes. (A) Morphological analysis of OB-loaded liposomes by transmission electron microscope (scale bar: 200 nm). (B-C) Size distribution and of Zeta potential distribution of OB-loaded liposomes determined by a Nano ZS90 Zetasizer. (D) Fluorescence imaging of MPTP-modeled C57BL/6J mice at 12 hours after intravenous injection of Lip, Lip-PEG, Lip-cRGD, or Lip-PEG-cRGD. Figure S2. Screening of MPP⁺ concentration and lip OB administration time window used in in vitro studies. (A) PC12 cells were exposed to different concentrations of MPP⁺. Twenty-four hours later, 5 μ M MPP⁺ reduced the cell viability to 60% ($n = 5$). (B-D) PC12

cells were pretreated with lip OB for the indicative time and then exposed to $5\ \mu\text{M}$ MPP⁺ for another 24 h. The LC3-II/LC3-I ratio and P62 expression were quantified using the western blotting. The OB (6 h) group displayed a better effect on activating autophagy ($n=3$). Data were expressed as means \pm SD. * $P < 0.05$, ** $P < 0.01$ compared with the control group. Figure S3. Transfection efficiency of PINK1 siRNA. PC12 cells were transfected with PINK1 siRNA for 12 h, and then the western blot assay was performed. PINK1 siRNA caused a significant decrease in PINK1 expression. Data were expressed as means \pm SD. ** $P < 0.01$ compared with Scramble siRNA group. (*Supplementary Materials*)

References

- [1] J. A. Obeso, M. Stamelou, C. G. Goetz et al., "Past, present, and future of Parkinson's disease: a special essay on the 200th Anniversary of the Shaking Palsy," *Movement Disorders*, vol. 32, no. 9, pp. 1264–1310, 2017.
- [2] Z. L. Ren, C. D. Wang, T. Wang et al., "Ganoderma lucidum extract ameliorates MPTP-induced parkinsonism and protects dopaminergic neurons from oxidative stress via regulating mitochondrial function, autophagy, and apoptosis," *Acta Pharmacologica Sinica*, vol. 40, no. 4, pp. 441–450, 2019.
- [3] Y. A. Sidorova, K. P. Volcho, and N. F. Salakhutdinov, "Neuroregeneration in Parkinson's disease: from proteins to small molecules," *Current Neuropharmacology*, vol. 17, no. 3, pp. 268–287, 2019.
- [4] A. Bose and M. F. Beal, "Mitochondrial dysfunction in Parkinson's disease," *Journal of Neurochemistry*, vol. 139, no. S1, pp. 216–231, 2016.
- [5] A. Camilleri and N. Vassallo, "The centrality of mitochondria in the pathogenesis and treatment of Parkinson's disease," *CNS Neuroscience and Therapeutics*, vol. 20, no. 7, pp. 591–602, 2014.
- [6] Y. Luo, A. Hoffer, B. Hoffer, and X. Qi, "Mitochondria: a therapeutic target for Parkinson's disease?" *International Journal of Molecular Sciences*, vol. 16, no. 9, pp. 20704–20730, 2015.
- [7] A. Bender, K. J. Krishnan, C. M. Morris et al., "High levels of mitochondrial DNA deletions in substantia nigra neurons in aging and Parkinson disease," *Nature Genetics*, vol. 38, no. 5, pp. 515–517, 2006.
- [8] B. R. De Miranda, S. L. Castro, E. M. Rocha, C. R. Bodle, K. E. Johnson, and J. T. Greenamyre, "The industrial solvent trichloroethylene induces LRRK2 kinase activity and dopaminergic neurodegeneration in a rat model of Parkinson's disease," *Neurobiology of Disease*, vol. 153, Article ID 105312, 2021.
- [9] K. R. Parzych and D. J. Klionsky, "An overview of autophagy: morphology, mechanism, and regulation," *Antioxidants and Redox Signaling*, vol. 20, no. 3, pp. 460–473, 2014.
- [10] R. Guan, W. Zou, X. Dai et al., "Mitophagy, a potential therapeutic target for stroke," *Journal of Biomedical Science*, vol. 25, no. 1, p. 87, 2018.
- [11] C. Yan, L. Gong, L. Chen et al., "PHB2 (prohibitin 2) promotes PINK1-PRKN/Parkin-dependent mitophagy by the PARL-PGAM5-PINK1 axis," *Autophagy*, vol. 16, no. 3, pp. 419–434, 2020.
- [12] A. M. Pickrell and R. J. Youle, "The roles of PINK1, parkin, and mitochondrial fidelity in Parkinson's disease," *Neuron*, vol. 85, no. 2, pp. 257–273, 2015.
- [13] J. Liu, W. Liu, R. Li, and H. Yang, "Mitophagy in Parkinson's disease: from pathogenesis to treatment," *Cells*, vol. 8, no. 7, p. 712, 2019.
- [14] A. B. Malpartida, M. Williamson, D. P. Narendra, R. Wade-Martins, and B. J. Ryan, "Mitochondrial dysfunction and mitophagy in Parkinson's disease: from mechanism to therapy," *Trends in Biochemical Sciences*, vol. 46, no. 4, pp. 329–343, 2021.
- [15] B. Almeida, O. K. Nag, K. E. Rogers, and J. B. Delehanty, "Recent progress in bioconjugation strategies for liposome-mediated drug delivery," *Molecules*, vol. 25, no. 23, p. 5672, 2020.
- [16] M. K. Yeh, M. K. Yeh, and Ming-Yen Cheng, "Clinical development of liposome-based drugs: formulation, characterization, and therapeutic efficacy," *International Journal of Nanomedicine*, vol. 7, pp. 49–60, 2011.
- [17] B. Kasenda, D. König, M. Manni et al., "Targeting immunoliposomes to EGFR-positive glioblastoma," *ESMO Open*, vol. 7, no. 1, Article ID 100365, 2022.
- [18] N. Zhang, F. Yan, X. Liang et al., "Localized delivery of curcumin into brain with polysorbate 80-modified cerasomes by ultrasound-targeted microbubble destruction for improved Parkinson's disease therapy," *Theranostics*, vol. 8, pp. 2264–2277, 2018.
- [19] F. Peng, L. Lu, F. Wei, D. Wu, K. Wang, and J. Tang, "The onjisaponin B metabolite tenuifolin ameliorates dopaminergic neurodegeneration in a mouse model of Parkinson's disease," *NeuroReport*, vol. 31, no. 6, pp. 456–465, 2020.
- [20] X. Li, J. Cui, Y. Yu et al., "Traditional Chinese nootropic medicine Radix Polygalae and its active constituent onjisaponin B reduce beta-amyloid production and improve cognitive impairments," *PLoS One*, vol. 11, no. 3, Article ID e0151147, 2016.
- [21] H. Li, J. Kim, H. N. K. Tran et al., "Extract of polygala tenuifolia, angelica tenuissima, and dimocarpus longan reduces behavioral defect and enhances autophagy in experimental models of Parkinson's disease," *NeuroMolecular Medicine*, vol. 23, no. 3, pp. 428–443, 2021.
- [22] A. G. Wu, V. K. Wong, S. W. Xu et al., "Onjisaponin B derived from Radix Polygalae enhances autophagy and accelerates the degradation of mutant alpha-synuclein and huntingtin in PC-12 cells," *International Journal of Molecular Sciences*, vol. 14, no. 11, pp. 22618–22641, 2013.
- [23] F. H. Sterky, A. F. Hoffman, D. Milenkovic et al., "Altered dopamine metabolism and increased vulnerability to MPTP in mice with partial deficiency of mitochondrial complex I in dopamine neurons," *Human Molecular Genetics*, vol. 21, no. 5, pp. 1078–1089, 2012.
- [24] Q. Hu and G. Wang, "Mitochondrial dysfunction in Parkinson's disease," *Translational Neurodegeneration*, vol. 5, no. 1, p. 14, 2016.
- [25] H. Tsukada, M. Kanazawa, H. Ohba, S. Nishiyama, N. Harada, and T. Kakiuchi, "PET imaging of mitochondrial complex I with 18F-BCPP-EF in the brains of MPTP-treated monkeys," *Journal of Nuclear Medicine*, vol. 57, no. 6, pp. 950–953, 2016.
- [26] A. H. Schapira, J. M. Cooper, D. Dexter, P. Jenner, J. B. Clark, and C. D. Marsden, "Mitochondrial complex I deficiency in Parkinson's disease," *The Lancet*, vol. 333, no. 8649, p. 1269, 1989.
- [27] Q. Lin, S. Li, N. Jiang et al., "PINK1-parkin pathway of mitophagy protects against contrast-induced acute kidney injury via decreasing mitochondrial ROS and NLRP3 inflammasome activation," *Redox Biology*, vol. 26, Article ID 101254, 2019.

- [28] J. F. Bion, I. H. Wilson, and P. A. Taylor, "Transporting critically ill patients by ambulance: audit by sickness scoring," *British Medical Journal*, vol. 296, no. 6616, p. 170, 1988.
- [29] O. A. Mareninova, W. Jia, S. R. Gretler et al., "Transgenic expression of GFP-LC3 perturbs autophagy in exocrine pancreas and acute pancreatitis responses in mice," *Autophagy*, vol. 16, no. 11, pp. 2084–2097, 2020.
- [30] A. R. Issa, J. Sun, C. Petitgas et al., "The lysosomal membrane protein LAMP2A promotes autophagic flux and prevents SNCA-induced Parkinson disease-like symptoms in the *Drosophila* brain," *Autophagy*, vol. 14, no. 11, pp. 1898–1910, 2018.
- [31] M. Pajares, A. I Rojo, G. Manda, L. Bosca, A. Cuadrado, and A. Cuadrado, "Inflammation in Parkinson's disease: mechanisms and therapeutic implications," *Cells*, vol. 9, no. 7, p. 1687, 2020.
- [32] Z. D. Zhou, S. P. Xie, W. T. Saw et al., "The therapeutic implications of tea polyphenols against dopamine (DA) neuron degeneration in Parkinson's disease (PD)," *Cells*, vol. 8, p. 911, 2019.
- [33] G. Li, J. Yu, L. Zhang, Y. Wang, C. Wang, and Q. Chen, "Onjisaponin B prevents cognitive impairment in a rat model of D-galactose-induced aging," *Biomedicine & Pharmacotherapy*, vol. 99, pp. 113–120, 2018.
- [34] L. Wen, N. Xia, P. Tang et al., "The gastrointestinal irritation of polygala saponins and its potential mechanism in vitro and in vivo," *BioMed Research International*, vol. 2015, Article ID 918048, pp. 1–8, 2015.
- [35] J. S. Bhatti, G. K. Bhatti, and P. H. Reddy, "Mitochondrial dysfunction and oxidative stress in metabolic disorders- a step towards mitochondria based therapeutic strategies," *Biochimica et Biophysica Acta- Molecular Basis of Disease*, vol. 1863, no. 5, pp. 1066–1077, 2017.
- [36] S. R. Subramaniam and M. F. Chesselet, "Mitochondrial dysfunction and oxidative stress in Parkinson's disease," *Progress in Neurobiology*, vol. 106–107, pp. 17–32, 2013.
- [37] A. Grunewald, K. R. Kumar, and C. M. Sue, "New insights into the complex role of mitochondria in Parkinson's disease," *Progress in Neurobiology*, vol. 177, pp. 73–93, 2019.
- [38] A. H. Schapira, "Mitochondria in the aetiology and pathogenesis of Parkinson's disease," *The Lancet Neurology*, vol. 7, no. 1, pp. 97–109, 2008.
- [39] P. Jenner, "Oxidative stress in Parkinson's disease," *Annals of Neurology*, vol. 53, no. S3, pp. S26–S38, 2003.
- [40] J. Geng, W. Liu, J. Gao et al., "Andrographolide alleviates Parkinsonism in MPTP-PD mice via targeting mitochondrial fission mediated by dynamin-related protein 1," *British Journal of Pharmacology*, vol. 176, no. 23, pp. 4574–4591, 2019.
- [41] L. Montava-Garriga and I. G. Ganley, "Outstanding questions in mitophagy: what we do and do not know," *Journal of Molecular Biology*, vol. 432, no. 1, pp. 206–230, 2020.
- [42] A. Eiyama and K. Okamoto, "PINK1/Parkin-mediated mitophagy in mammalian cells," *Current Opinion in Cell Biology*, vol. 33, pp. 95–101, 2015.
- [43] L. Barazzuol, F. Giamogante, M. Brini, and T. Cali, "PINK1/Parkin mediated mitophagy, Ca(2+) signalling, and ER-mitochondria contacts in Parkinson's disease," *International Journal of Molecular Sciences*, vol. 21, no. 5, p. 1772, 2020.
- [44] T. Kitada, S. Asakawa, N. Hattori et al., "Mutations in the parkin gene cause autosomal recessive juvenile parkinsonism," *Nature*, vol. 392, no. 6676, pp. 605–608, 1998.
- [45] E. M. Valente, P. M. Abou-Sleiman, V. Caputo et al., "Hereditary early-onset Parkinson's disease caused by mutations in PINK1," *Science*, vol. 304, no. 5674, pp. 1158–1160, 2004.
- [46] Y. Xu, F. Zhi, J. Mao et al., " δ -opioid receptor activation protects against Parkinson's disease-related mitochondrial dysfunction by enhancing PINK1/Parkin-dependent mitophagy," *Aging (Albany NY)*, vol. 12, no. 24, pp. 25035–25059, 2020.
- [47] C. Y. Huang, K. Sivalingam, M. A. Shibu et al., "Induction of autophagy by vasicinone protects neural cells from mitochondrial dysfunction and attenuates paraquat-mediated Parkinson's disease associated alpha-synuclein levels," *Nutrients*, vol. 12, no. 6, p. 1707, 2020.
- [48] H. Wang, X. Xu, X. Guan et al., "Liposomal 9-aminoacridine for treatment of ischemic stroke: from drug discovery to drug delivery," *Nano Letters*, vol. 20, no. 3, pp. 1542–1551, 2020.
- [49] X. Han, S. Zhao, H. Song et al., "Kaempferol alleviates LD-mitochondrial damage by promoting autophagy: implications in Parkinson's disease," *Redox Biology*, vol. 41, Article ID 101911, 2021.
- [50] Y. Chen, Q. S. Zhang, Q. H. Shao et al., "NLRP3 inflammasome pathway is involved in olfactory bulb pathological alteration induced by MPTP," *Acta Pharmacologica Sinica*, vol. 40, no. 8, pp. 991–998, 2019.
- [51] B. H. Tran, Y. Yu, L. Chang et al., "A novel liposomal S-Propargyl-Cysteine: a sustained release of hydrogen sulfide reducing myocardial fibrosis via TGF- β 1/smad pathway," *International Journal of Nanomedicine*, vol. 14, pp. 10061–10077, 2019.
- [52] J. Ren, Z. Pei, X. Chen et al., "Inhibition of CYP2E1 attenuates myocardial dysfunction in a murine model of insulin resistance through NLRP3-mediated regulation of mitophagy," *Biochimica et Biophysica Acta- Molecular Basis of Disease*, vol. 1865, no. 1, pp. 206–217, 2019.